NASA CR-132660

25373

A STUDY OF THE DIFFUSIONAL BEHAVIOR OF A TWO-PHASE METAL MATRIX COMPOSITE EXPOSED TO A HIGH TEMPERATURE ENVIRONMENT

D. R. Tenney
Principal Investigator

Metallurgical Engineering
Division of Minerals Engineering

Final Report

Prepared under Grant No. NGR 47-004-097 by
VIRGINIA POLYTECHNIC INSTITUTE & STATE UNIVERSITY
Blacksburg, Virginia

for

NATIONAL AERONAUTICS AND SPACE ADMINISTRATION

TABLE OF CONTENTS

	Page
Introduction	1
Mathematical Model	3
Theoretical Analysis	4
Numerical Analysis	6
Concentration Expressed as Volume Fraction	12
Composition Profiles Between First and Second Nearest Neighbor Filaments	13
Materials and Procedures	16
Fabrication of Wire Specimens	17
Results and Discussions	19
Summary and Conclusions	34
List of Figure Captions	35
References	36

ABSTRACT

The progress of diffusion-controlled filament-matrix interaction in a metal matrix composite where the filaments and matrix comprise a two-phase binary alloy system was studied by mathematically modeling compositional changes resulting from prolonged elevated temperature exposure. The analysis treats a finite, diffusion-controlled, two-phase moving-interface problem by means of a variable-grid finite-difference technique. The Ni-W system was selected as an example system. Modeling was carried out for the 1000° to 1200°C temperature range for unidirectional composites containing from 6 to 40 volume percent tungsten filaments in a Ni matrix. The results are displayed to show both the change in filament diameter and matrix composition as a function of exposure time. Compositional profiles produced between first and second nearest neighbor filaments were calculated by superposition of finite-difference solutions of the diffusion equations, and by direct finite difference calculation employing symmetry point boundary conditions. Results showing the decrease in filament volume fraction with exposure time are presented for composites containing initially different filament volume fractions. Curves illustrating the effect of filament diameter on the rate of decrease of the filament volume fraction are also presented.

INTRODUCTION

Elevated temperature exposure of a metal matrix composite may produce compositional and microstructural changes which result in degradation of composite properties. The extent of these changes will depend on the severity of the exposure conditions, the nature of the components, and type of interfacial reactions which occur. A general scheme for classification of composite system according to the type of interfacial reactions which occur has been suggested by Metcalf[1]. The three classes which have been proposed are:

Class I. Filament and matrix mutually non-reactive and insoluble.

Class II. Filament and matrix mutually non-reactive but soluble.

Class III. Filament and matrix react to form chemical compound(s) at the interface.

Although clear cut definitions between these classes are not always possible, this scheme of grouping provides a systematic background against which to consider their characteristics. Composite systems which belong to Class II are more susceptible to diffusional interaction than those which belong to either of the other two classes of composites. Class II systems can be further subdivided into three identifiable subclasses as follows:

II. (a) Filaments and matrix exhibit complete solid solubility.

(b) Filaments and matrix exhibit limited solid solubility with no intermediate phases.

(c) Filament and matrix react to form an intermediate phase between the filament and matrix phases.

An analytical technique for calculating compositional changes in Class II(a) composites has been previously[2] developed. This paper reports the results of a research program designed to develop a similar analysis for modeling the compositional changes produced by diffusion between the filaments and matrix for a two-phase composite system of type II(b). A finite difference analysis employing a variable grid technique[3] similar to that developed by Tranzilli and Heckel[4,5] for homogenization studies has been utilized to solve the appropriate diffusion equations. The Ni-W system has been examined as a model Class II(b) two-phase composite system. Changes in filament diameter and compositional changes in the Ni matrix have been calculated as a function of exposure time. Results illustrating the influence of initial filament volume fraction and initial filament diameter on rate of change of filament volume fraction at 1000°, 1100°, and 1200°C are presented.

MATHEMATICAL MODEL

The mathematical modeling of filament/matrix interaction will be performed for an idealized composite which contains the symmetrical arrangement of filaments depicted in Figure 1. Filaments are assumed to exist in the form of parallel right circular cylinders embedded in a matrix of differing material. The arrangement shown in Figure 1 corresponds to a 40 volume percent filament composite with the filaments arranged so as to give a hexagonal stacking on a cross-section perpendicular to the long axis of the filaments. They are periodically spaced so that the entire filament array can be described by specifying the filament locations with the basic symmetry element shown in the lower part of the figure. By repeating this element along the axis directions corresponding to the sides of the element, packed face-to-face, the entire composite cross-section can be constructed. Therefore, in order to completely describe the compositional changes which occur in the composite as a result of high temperature exposure it is necessary only to describe the changes which take place in the symmetry element. The composition at any point within the symmetry element can be approximated for given diffusion conditions by assuming that the contributions from neighboring filaments are additive. This requires that the contributions from all filaments which are sufficiently close to give a significant contribution be summed. In general, the primary contributors will be the four closest filaments. This method of analysis provides very satisfactory results for cases where there is a small to moderate amount of overlap of composition profiles emanating from the different filaments. However, for cases where there is extensive profile overlap or a large degree

of filament/filament interaction, the predicted results are subject to considerable inaccuracy. This latter case would correspond to the condition where the matrix between filaments is nearing saturation.

Since we were more interested in the early stages of filament/matrix interaction than in the latter stages, the method of superposition has been employed in this study. An alternate method involving direct finite difference calculation of the matrix composition profiles has also been employed for those cases where suitable boundary conditions could be defined from symmetry considerations. This method, where applicable, does yield accurate results even for long term exposure conditions which product extensive interaction in the matrix. These methods will be further considered in a later section after the finite-difference analysis for solution of the diffusion equations has been developed.

Theoretical Analysis

To solve for the change in concentration with distance from the center of a filament in a composite system where the filaments and matrix show limited solid solubility, a variable-grid finite-difference technique will be employed. Diffusion in such a two-phase system can be described by a set of coupled partial differential equations expressed in the form:

$$\frac{\partial c^{\alpha}}{\partial t} = \frac{1}{r}\frac{\partial}{\partial r}\left(rD^{\alpha}(c)\frac{\partial c^{\alpha}}{\partial r}\right) \qquad (\alpha\text{-phase}) \qquad (1)$$

and

$$\frac{\partial c^{\beta}}{\partial t} = \frac{1}{r}\frac{\partial}{\partial r}\left(rD^{\beta}(c)\frac{\partial c^{\beta}}{\partial r}\right) \qquad (\beta\text{-phase}) \qquad (2)$$

where $D^{\alpha}(c)$ and $D^{\beta}(c)$ are the concentration dependent interdiffusion coefficients in the α and β phases. Flux considerations based on a diffusion controlled

reaction show that at the interface, the mass balance condition is:

$$(C_{\beta\alpha} - C_{\alpha\beta}) \frac{d(\epsilon/2)}{dt} = D^{\alpha}(C_{\alpha\beta})\left(\frac{dC^{\alpha}}{dr}\right)_{r=\epsilon^{+}/2} - D^{\beta}(C_{\beta\alpha})\left(\frac{dC^{\beta}}{dr}\right)_{r=\epsilon^{-}/2} \quad (3)$$

where $C_{\beta\alpha}$ and $C_{\alpha\beta}$ are the concentrations at the interface in the β and α phases, $\epsilon/2$ is the position of the interface, and $\left(\frac{dC^{\alpha}}{dr}\right)_{r=\epsilon^{+}/2}$ and $\left(\frac{dC^{\beta}}{dr}\right)_{r=\epsilon^{-}/2}$ are the concentration gradients at the interface in the α and β phases, respectively. The meaning of these terms can best be understood by reference to Figure 1 where a schematic cross-section of a diffused specimen is shown. The concentration in the sample is plotted as a function of distance from the center of the filament $r = 0$ to a distance $L/2$ in the surrounding matrix phase. The β-phase region corresponding to the filament extends from $r_o = 0$ to $r_I = \epsilon/2$ and the α-phase region corresponding to the surrounding matrix extends from $r_I = \epsilon/2$ to $r_N = L/2$. The initial and boundary conditions to be satisfied are:

Initial conditions:

$C = 1.0$ for $0 \leq r \leq \epsilon/2$, $t = 0$

$C = 0.0$ for $\epsilon/2 \leq r \leq L/2$, $t = 0$

Boundary conditions:

$C = C_{\beta\alpha}$ at $r = \epsilon^{-}/2$, $t > 0$

$C = C_{\alpha\beta}$ at $r = \epsilon^{+}/2$, $t > 0$

$\left(\frac{dC^{\beta}}{dr}\right) = 0$ at $r = 0$ and $r = r_1$, $t > 0$

$\left(\frac{dC^{\alpha}}{dr}\right) = 0$ at $r = L/2$, $t > 0$

where $\epsilon^{-}/2$ and $\epsilon^{+}/2$ refer to the β and α sides of the interface. Further consideration of these boundary conditions will be given in the following section.

Numerical Analysis

A variable grid finite difference technique will be employed to numerically solve the diffusion equations presented above. The Murray-Landis[3] variable space grid transformation to be used can best be illustrated by again considering the schematic sample cross-section shown in Figure 2. The α-phase is divided into N-I equally sized space increments of thickness Δr^{α}. The β-region is divided into I space increments all of which are Δr^{β} thick except the first increment which is selected to be of thickness r_1. The value of r_1 is taken to be equal to either Δr_{β} or to $\epsilon/2 - r_D$ where r_D is the estimated diffusion zone thickness in the β-phase for the total time being considered. If $r_D \geq \epsilon/2$, then r_1 is set equal to Δr_{β}. This case would be realized for very high temperature diffusion with small diameter filaments. If, however, r_D is significantly less than $\epsilon/2$, then $r_1 = \epsilon/2 - r_D$. This case would be realized for lower temperature diffusion with larger diameter filaments. The reason for defining r_1 in this manner for the latter case is to concentrate the grid points for the finite-difference analysis in the region immediately adjacent to the interface where the significant diffusional changes are occurring. The location corresponding to r_1 must, however, be treated as a "floating" boundary condition. If the diffusion solution is carried out to a time when the composition ar r_1 starting varying from 1.0, it would be necessary to stop the analysis and redefine a new grid in the β-phase with a smaller r_1 before proceeding. This is required because accurate compositional changes can not be calculated at r_1 due to the large difference in grid size on either side of this location. More will be said about this method for concentrating grid points in the region near the interface for small diffusion zones corresponding to short times or lower temperatures in a later section dealing with accuracy and stability.

If the α/β interface moves with diffusion time, the thicknesses of the α- and β-phases will also change. Since the number of stations in each phase remains constant, the grid spacing Δr must change with time. The location of an internal point is thus always a constant percentage of the instantaneous phase thickness.

The rate of travel of any point is related to the velocity of the interface by:

$$\frac{dr_n}{dt} = \frac{r_n}{(\epsilon/2)} \frac{d(\epsilon/2)}{dt} \tag{4}$$

Thus the rate of change of concentration at any internal station can be expressed as:

$$\frac{dC_n}{dt} = \frac{\partial C_n}{\partial r_n} \left(\frac{dr_n}{dt}\right) + \frac{\partial C_n}{\partial t} \tag{5}$$

where $\frac{\partial C_n}{\partial t}$ is given by Fick's Second Law. By combining Equations (4) and (5), an expression for the variation of concentration with time at an internal station, n, in the β-phase can be written as follows:

$$\frac{dC_n^\beta}{dt} = \frac{r_n}{(\epsilon/2)} \frac{\partial C_n^\beta}{\partial r_n} \frac{d(\epsilon/2)}{dt} + \frac{\partial C_n^\beta}{\partial t} \tag{6}$$

In analogous fashion, the change in concentration with time at an internal station, n, in the α-phase relative to the stationary α-phase boundary at $r = L/2$ is given by:

$$\frac{dC^\alpha}{dt} = \left(\frac{L/2 - r_n}{L/2 - \epsilon/2}\right) \frac{\partial C_n^\alpha}{\partial r_n} \frac{d(\epsilon/2)}{dt} + \frac{\partial C_n^\alpha}{\partial t} \tag{7}$$

Before developing the finite difference expressions for the above equations, it is mathematically convenient to make a change of variables so that all

variables will be normalized. This can be accomplished by making use of the following change of variables:

$$R = \frac{r}{L/2}\ , \quad T = \frac{D^{\alpha}_{max}\, t}{(L/2)^2}, \quad \overline{D^{\alpha}}(C) = \frac{D^{\alpha}(C)}{D^{\alpha}_{max}}, \quad \overline{D^{\beta}}(C) = \frac{D^{\beta}(C)}{D^{\beta}_{max}}$$

where D^{α}_{max} and D^{β}_{max} are the maximum values of the concentration dependent diffusion coefficients in the α-phase and in the β-phase. All other parameters have their usual meaning. Using these definitions, R becomes the normalized distance, T the normalized time, $\overline{D^{\alpha}}(C)$ and $\overline{D^{\beta}}(C)$ normalized diffusion coefficients in the α- and β-phases. It is also convenient to make the following additional definitions:

$$\delta = C_{\beta\alpha} - C_{\alpha\beta}$$

$$\emptyset = D^{\beta}_{max}/D^{\alpha}_{max}$$

and $$\lambda = (C_{\beta 0} - C_{\beta\alpha})/(C_{\alpha\beta} - C_{\alpha 0})$$

where $C_{\beta 0}$ and $C_{\alpha 0}$ are the initial concentrations of the β- and α-phases at time $t = 0$. Using the normalizing expressions for R, T, $\overline{D^{\alpha}}(C)$ and $\overline{D^{\beta}}(C)$, Equations (1), (2), and (3) can be rewritten to give:

$$\frac{\partial C^{\alpha}}{\partial T} = \overline{D^{\alpha}}(C)\left[1/R\ \frac{\partial C^{\alpha}}{\partial R} + \frac{\partial^2 C^{\alpha}}{\partial R^2}\right] + \frac{\partial \overline{D^{\alpha}}(C)}{\partial R}\ \frac{\partial C^{\alpha}}{\partial R} \tag{8}$$

$$\frac{\partial C^{\beta}}{\partial T} = \emptyset\left[\overline{D^{\beta}}(C)\ \left(1/R\ \frac{\partial C^{\beta}}{\partial R} + \frac{\partial^2 C^{\beta}}{\partial R^2}\right) + \frac{\partial \overline{D^{\beta}}}{\partial R}\ \frac{\partial C^{\beta}}{\partial R}\right] \tag{9}$$

and $$\delta\frac{d(\epsilon/2)}{dT} = (L/2)\left[\overline{D^{\alpha}_{\alpha\beta}}\left(\frac{dC^{\alpha}}{dR}\right)_{r=\epsilon^{+}/2} - \emptyset\ \overline{D^{\beta}_{\beta\alpha}}\left(\frac{dC^{\beta}}{dR}\right)_{r=\epsilon^{-}/2}\right] \tag{10}$$

The interface mass balance given by Eq. (10) couples Eqs. (8) and (9) and can be solved for the interface velocity.

Rewriting the above equations in finite difference form leads to the following expressions:

(α-phase)

$$\frac{C_n^{j+1} - C_n^{j}}{\Delta T} = \left(\frac{1-R_n}{L/2 - \epsilon/2}\right) \frac{(C_{n+1}^{j} - C_{n-1}^{j})}{2\Delta R_n^{\alpha}} \frac{d(\epsilon/2)}{dT} + \frac{\partial C_n^{\alpha}}{\partial T} \tag{11}$$

where

$$\frac{\partial C_n^{\alpha}}{\partial T} = \overline{D^{\alpha}}(C) \left[\frac{1}{R_n} \frac{(C_{n+1}^{j} - C_{n-1}^{j})}{2\Delta R^{\alpha}} + \frac{(C_{n+1}^{j} - 2C_n^{j} + C_{n-1}^{j})}{(\Delta R^{\alpha})^2}\right] +$$

$$\frac{(\overline{D^{\alpha}}_{n+1} - \overline{D^{\alpha}}_{n-1})}{2\Delta R_n} \frac{(C_{n+1}^{j} - C_{n-1}^{j})}{2\Delta R^{\alpha}} \tag{12}$$

For the β-phase we have:

$$\frac{C_n^{j+1} - C_n^{j}}{\Delta T} = \frac{R_n}{\epsilon/2} \frac{d(\epsilon/2)}{dT} \frac{(C_{n+1}^{j} - C_{n-1}^{j})}{2\Delta R} + \frac{\partial C_n^{\beta}}{\partial T} \tag{13}$$

where

$$\frac{\partial C_n^{\beta}}{\partial T} = \emptyset \left\{ \overline{D^{\beta}}_n \left[\frac{1}{R_n^{\beta}} \frac{(C_{n+1}^{j} - C_{n-1}^{j})}{2\Delta R^{\beta}} + \frac{(C_{n+1} - 2C_n^{j} + C_{n-1}^{j})}{(\Delta R^{\beta})^2} \right] +$$

$$\frac{(\overline{D^{\beta}}_{n+1} - \overline{D^{\beta}}_{n-1})}{2\Delta R^{\beta}} \frac{(C_{n+1}^{j} - C_{n-1}^{j})}{2\Delta R^{\beta}} \tag{14}$$

The finite difference expression for the interface mass balance equation is given by:

$$\frac{d(\epsilon/2)}{dt} = (L/2)(1/\delta)\left[\overline{D^{\alpha}_{\alpha\beta}} \frac{(-C_{I+2}^{j} + 4C_{I+1}^{j} - 3C_{\alpha\beta}^{j})}{2\Delta R^{\alpha}} - \emptyset \overline{D^{\beta}_{\beta\alpha}} \frac{(C_{I-2}^{j} - 4C_{I-1}^{j} + 3C_{\beta\alpha}^{j})}{2\Delta R^{\beta}} \right. \tag{15}$$

It can readily be shown that in finite difference notation the correct form of Eq. (13) at station n = 1 corresponding to the center of the β-filament is given by

$$\frac{(C_1^{j+1} - C_1^{j})}{\Delta T} = 4\emptyset \, \overline{D}_1^{\beta} \frac{(C_2^{j} - C_1^{j})}{(\Delta R^{\beta})^2} \qquad (15)$$

In analogous fashion it can be shown that the correct form of Eq. (11) at station n = N corresponding to the outer boundary condition at R = 1 (r = L/2) is given by:

$$\frac{(C_N^{j+1} - C_N^{j})}{\Delta T} = 2\overline{D}_N^{\alpha} \frac{(C_{N-1}^{j} - C_N^{j})}{(\Delta R^{\alpha})^2}$$

In order to solve the above equations, a general computer program was developed. Information which must be input into this program included concentration dependent diffusion coefficients, solubility limits of each phase, initial filament diameter and symmetry element dimensions which determine boundary conditions, molal volumes of Ni and W, number of stations to be set up in each phase, estimated diffusion distance, r_D, in the β-phase, diffusion temperature, desired analysis times, and other required control parameters. Calculated diffusion solutions were printed out and plotted on a Calcomp plotter for ease of viewing. The solutions for different times could be each plotted on separate graphs or all plotted on the same graph to facilitate comparison. The amount the filament/matrix interface shifted with diffusion time, t, was also calculated and output. For each solution a mass balance calculation was performed to check for conservation of mass. As an additional check on solution stability, a test case was considered in which the grid

sizes in the filament and matrix were varied in an effort to establish the optimum grid size for which a convergent solution of acceptable accuracy could be obtained. A stable solution was defined as one for which the shift of the filament/matrix interface, at a given time, remained unchanged (less than 2 percent variation) as the grid size approached zero, $\Delta r \rightarrow 0$. Calculations were performed for a sample with a 50 μm thick Ni layer. Exposure conditions were selected to be 1200^{o}C for 10 hours. Because the interdiffusion coefficients in the W-filament (β-phase) were much smaller than those in the Ni-matrix (α-phase), the motion of the interface is primarily controlled by diffusion in the matrix. For this reason the initial grid size in the filament was selected to be 0.5 μm while the grid size in the matrix was varied from 2 μm to 0.05 μm. On plotting the interface shift as a function of matrix grid size, a nearly linear relationship was found to exist except at very small values of Δr where the relative position of the interface tended toward a constant value. By selecting an 0.5 μm grid size, the error in the interface position determined by comparing with the true interface position obtained by extrapolating to $\Delta r = 0$ was less than 2%. The difference between the true and actual position of the interface for longer times was found to remain essentially constant. Thus for these runs an 0.5 μm initial grid size in the α-phase was selected as giving a reasonable compromise between solution accuracy and computer time.

In addition to specifying the optimum grid size, it is also necessary to specify a time increment which gives a stable and non-oscillatory solution. For the numerical analysis used, the time increment was selected such that $\Delta t \leq 1/4\ \Delta r^2/D^{\alpha}_{max}$ or $\Delta T \leq 1/4(\Delta R^{\alpha})^2$. A trade off between solution accuracy,

small ΔR, and minimum computer time, large ΔT, must always be made. One approach to obtaining good solution accuracy while holding down the computation time is to start the analysis with a small grid size and them increase the grid size when the diffusion zone has grown to a predetermined size. For long solution times, one or more grid size changes may be required if computer time is held to a minimum without undue compromise in solution accuracy. The computer program developed for this study has been designed to permit any number of changes in grid size.

Concentration Expressed as Volume Fraction

It should be noted that no correction for variation in molal volume has been included in the above analysis. However, in the Ni-W system there is approximately a 27 percent difference in the molal volumes of the pure metals which, if not accounted for, would cause significant error[6] in the predicted results. Recently, Guy, DeHoff and Smith[7] have shown that if ideal solution behavior is assumed and the concentrations are defined in terms of volume fraction, the same form of Fick's law can be used with only minor computational refinements required. Concentration in terms of volume fraction, C_1, can be related to the more conventional atomic fraction, N_1, by the following relationship:

$$C_1 = \frac{\overline{V_1}}{V} N_1$$

where $\overline{V_1}$ is the partial molal volume of component 1 and V is the molal volume of the solid solution. Using the general relation $V = N_1\overline{V_1} + N_2\overline{V_2}$, the above equation becomes

$$C_1 = \frac{N_1\overline{V_1}}{\overline{V_2} + N_1(\overline{V_1} - \overline{V_2})}$$

By knowing the change in lattice parameter with composition for the Ni-rich region in the Ni-W system the variation of V with N_{Ni} can be calculated. A plot of V versus N_{Ni} for this region showed that a nearly linear relationship existed between these two quantities. Suitable choices of $\bar{V}_{Ni}$ and $\bar{V}_{W}$ slightly different than the molal volumes of the pure metals produced a good linear approximation to the central experimental values. The values used were $\bar{V}_{Ni}$ = 6.55 and $\bar{V}_{W}$ = 8.93. The procedure used was to express the concentration in terms of volume fraction for the computations and then convert it back to atomic fraction once the desired solution had been calculated.

Composition Profiles Between First and Second Nearest Neighbor Filaments

As pointed out in an earlier section by employing the principle of superposition it is possible to calculate the compositional changes which occur at any point within the symmetry element shown in Figure 1. For the sake of simplicity, however, solutions will be calculated only along the lines connecting centers of first nearest neighbor filaments (sides and short diagonal of the symmetry element) and along the line connecting second nearest neighbor filaments (long body diagonal of symmetry element). Because of the symmetry found in these directions, certain simplifying assumptions can be made.

To facilitate calculation of the profile between first nearest neighbors, it will be assumed that the point midway between the filaments is a zero flux boundary condition. This allows a direct calculation of the profile for all exposure times without the necessity to employ superposition. For large filament sizes, such as those being considered in this study, this method of solution is believed to result in accurate profiles. It should be pointed out, however, that the assumption of a zero flux condition between filaments is not entirely

correct. For large degrees of interaction there will be a small loss of material from the central region between filaments due to diffusion down the concentration gradient perpendicular to the line connecting the filaments. However, since the gradient in the perpendicular direction is small, the net loss of material in that direction is small and will be assumed negligible for this analysis.

For hexagonal stacking of filaments, second nearest neighbor filaments are those located at the ends of the long body diagonal of the symmetry element shown in Figure 1. Two basically different methods can be used to calculate compositional changes along the body diagonal line connecting second nearest neighbor filaments. The simplest and most straight forward way is to superimpose the contributions of the filament located at the corners of the symmetry element. These four filaments are the primary contributors and the presence of other filaments located further from the body diagonal line can be neglected for all practical purposes. This method gives good results for low degrees of interaction but is not suitable for large degrees of interaction.

A second method for determining the compositional profiles between second nearest neighbors is to make use of the symmetry found along the body diagonal line to define boundary conditions which permit a direct finite difference calculation of the compositional changes over the end sections near the filaments. The remainder of the profile, over the center section, must then be calculated by superposition, or estimated. The rationale for this approach can best be understood by again referring to the hexagonal symmetry element shown in Figure 1. Points E and G are located at the centers of equilateral triangles ACD and ABC. Since point E is an equidistance from filaments A, C, and D, there will be an equal flux of W atoms from these filaments to

point E. There will be no flow of W atoms from this point which makes it a zero flux location. The flux of W atoms from filament D along line BD is identically balanced by the sum of the components of the fluxes from filaments A and C projected on line BD. A similar flux balance also exists at point G. Since the boundary conditions at these points can be defined, a direct finite difference calculation of the composition changes along the body diagonal line can be made for the region from the centers of the filaments on each end, B and D, to the minima points E and G. The profile over the center section from E to G can not be directly calculated. However, the composition at the very center, point F, can be determined by picking this point off the profile calculated between first nearest neighbor filaments A and C. Point F will be the maximum composition found over the central portion of the profile along the body diagonal. By knowing the values of the composition at the inflection points along line BD, the approximate shape of the composition contour over the central region can be obtained by simply drawing a smooth curve from the ends of the calculated end sections through the central maxima at F.

Alternate approaches to estimating the composition variation over the center region is to employ superposition of the contribution from the two closest filaments, A and C or from all four corner filaments. A discussion of the relative merits of each of these approximations will be given in a later section where profiles calculated by these methods are presented.

MATERIALS AND PROCEDURES

Test samples, approximately 2.0 cm in diameter by 2 cm long, were cut from a 15 cm long Ni-W composite cylinder. The Ni-W composite cylinder consisted of a central bundle of parallel, 0.16 mm diameter W-wires in a continuous matrix of pure Ni. This cylindrical specimen was fabricated at Batelle Columbus Laboratories by an isostatic hot pressing technique and was secured for this grant by Dr. H. W. Herring, Langley Research Center.

The test samples were cut from the cast cylinder and polished in such a way that their cross-sections could be microscopically observed. Two stages of sample etching were required to reveal the nickel and tungsten grain boundaries due to the ineffectiveness of any one etchant on both phases. Although several etchants for nickel were tried, a solution of 70% nitric acid and glacial acetic acid in equal proportions by volume produced the best grain boundary contrast. The tungsten was etched in a solution containing 300 grams per liter potassium ferricyanide and 100 grams per liter sodium hydroxide. A swab of two to three seconds at room temperature was sufficient to develop grain contrast for nickel or tungsten in their respective etchants.

Observation of the grain structure revealed a diffusion zone surrounding each tungsten filament indicating substantial initial diffusion of the tungsten into the nickel matrix. The W filaments also showed a recrystallized outer layer adjacent to the Ni resulting from diffusion of Ni into the W-wires during the high temperature hot pressing operation used to fabricate the specimens.

The initial concentration profile existing in the reaction zones surrounding the filaments was measured by quantitative electron microprobe analysis. The probe analysis was carried out using an ARL electron microprobe operated at 15 kV and 0.10 μ-amp beam current. The X-ray intensities of the NiK_α line and the WM_α line were simultaneously recorded using a constant beam current mode. Standards of pure Ni and pure W were employed along with Colby's Magic[8] microprobe correction program to convert the raw intensity data to concentrations in atomic percent. Colby's original program has been modified to make it more adaptable to correction of the continuous data collected in diffusion analysis. Also, a plot subroutine has been added to the program so that the computer plots the corrected concentration profiles.

Fabrication of Wire Specimens

An experimental effort is continuing to produce Ni-W composite wire specimens in an attempt to study the effect of diffusion on mechanical properties. The plan is to prepare composite specimens by electroplating Ni on W wires and then to tensile test these specimens after different lengths of exposure time at 1200°C. The change in filament diameter and concentration profile existing in the specimen after each exposure time will be theoretically simulated and experimentally confirmed. An attempt will then be made to find correlations between the degree of diffusion reaction and the measured changes in ultimate tensile strength.

In order to electroplate Ni on the W wires the first step was to prepare the surface of the W wires. The procedure used consisted of anodic etching of the filament in a solution of 300 grams per liter potassium ferricyanide and 100 grams per liter sodium hydroxide at room temperature using a current

density of 4.4 amps per square decimeter. The sample was then washed thoroughly in boiling distilled water and placed in a Wood's strike bath for twenty minutes. The composition of this bath consisted of 536 grams per liter nickel chloride and 125 ml hydrochloric acid. A current density of 4.4 amps per square decimeter was used. Finally the filaments were plated in an acid Watts bath at a current density of 2.2 amps per square decimeter and a temperature of 160^{o}F. The composition of the Watts bath was as follows: nickel sulfate 239.7 grams per liter, nickel chloride 44.9 grams per liter, and boric acid 29.9 grams per liter at a pH of 4.5. The Ni deposits thus produced look good but more research and testing is required to obtain the best possible deposits.

RESULTS AND DISCUSSIONS

Typical concentration profiles for diffusion between a 50 μm radius W-filament and surrounding Ni-matrix at 1200°C are shown in Figure 3. The atomic percent tungsten is plotted as a function of distance in microns from the center of the W-filament. Curves for exposure times of 10, 100, 200 and 500 hours are shown. It will be noted that the W/Ni interface moves into the W-filament with increasing exposure time. The direction of interface movement is inward because the flux of W atoms from the filament into the surrounding matrix is larger than the opposite flux of Ni atoms into the filament. The difference in mass flow can be attributed to two factors. First, the rates of diffusion in the Ni-rich phase are orders of magnitude higher than those in the W-rich phase. Secondly and more importantly is the fact that for the 1000° to 1200°C temperature range being considered in this study the solubility limit of Ni in W is only 0.9 atomic percent whereas the solubility limit of W in the Ni-rich phase is 17.1 atomic percent. Because of these two factors, the W/Ni interface will move into the W-filament with increasing exposure time until either the surrounding Ni matrix is saturated with W or the W-filament disappears. The amount by which the W-filaments will be reduced in diameter obviously depends on the volume fraction filaments in the composite. The higher the filament volume fraction the lower the matrix volume fraction and thus the smaller the amount of W necessary to saturate the matrix.

The results of Figure 3 basically depict the case of a single filament surrounded by an infinitely large matrix or a composite where the spacing between filaments is sufficiently large to prevent any interaction of profiles from neighboring filaments for the diffusion times being considered. This latter case would represent a composite of such low volume fraction filaments that it would not be of much interest from a practical view point. Let us, therefore, consider composites which contain from 20 to 50 volume percent filaments where the volume percent is high enough to be of some practical interest. For a reactive composite system such as the W-Ni system, prolonged high temperature exposure of high volume fraction filament composites (20 to 50%) would result in extensive interaction of profiles emanating from neighboring filaments. Composition profiles between centers of nearest neighbor filaments for a 20 and 40 volume percent W-filament Ni matrix composites are shown in Figure 4. The exposure conditions were 1200^{o}C for times of 10, 100, 200 and 500 hours. A hexagonal stacking of filaments has been assumed which means that for the 22 volume percent composite the filament-to-filament spacing is 2R and the center-to-center spacing is 4R. For the 40 volume percent composite the filament-to-filament spacing is 1R and the center-to-center spacing is 3R. These profiles were calculated by symmetry point analysis which assumes that a zero flux condition exists midway between the filaments thus allowing the profiles to be directly calculated by the finite difference technique discussed earlier. This method of calculation assumes that there is no loss of W from the center line connecting filaments due to diffusion perpendicular to this line. For relatively large filament diameters such as those being considered in this analysis, this is a reasonably good assumption.

The results presented in Figure 4 clearly show the effect of filament volume fraction on the distance the filament/matrix interface moves with exposure time. Since the filaments are closer in the 40 volume percent composite than in the 20 volume percent composite, the Ni matrix between filaments saturates quicker. Saturation halts the movement of the W/Ni interface. The concentration profile between filaments in the 40 volume percent composite will not change after 500 hours as the matrix is completely saturated. However, the interface position and build-up of W in the matrix of the 20 volume percent composite will continue to change with exposure times longer than 500 hours until which time as the matrix either reaches saturation or the filaments disappear.

The volume percent filaments in a composite determine how much each filament will be reduced in diameter before matrix saturation occurs. However, the rate at which a given composite proceeds toward matrix saturation is primarily determined by the exposure temperature. Figure 5 shows a comparison of nearest neighbor composition profiles for a 40 volume percent composite exposed at 1200°C and 1100°C for 200 hours. Although the difference in exposure temperature is only 100°C, it is large enough to result in a significant difference in the extent of interdiffusion. The W/Ni interface has moved more than twice as far at 1200°C as at 1100°C. This difference is also reflected in the relative amounts of W in the Ni matrix between filaments. Temperature is very important because the rates of atomic diffusion, which are rate controlling, are exponentially dependent on temperature.

In an earlier section, two basically different methods were discussed for calculating composition profiles between nearest neighbor filaments. These two methods have previously been referred to as (a) superposition and

(b) symmetry point analysis. A comparison of profiles calculated by these techniques is presented in Figure 6. Profiles calculated for a 500 hour exposure at 1200°C for a 22 volume percent and a 40 volume percent composite are shown. In both composites the initial radius of the W-filaments was 50 μm with a filament-to-filament spacing of 2R in the 22 volume percent composite and 1R in the 40 volume percent composite. In both graphs, the solid line curve was calculated by symmetry point analysis while the curve marked with solid circles was calculated by superposition. For the 22 volume percent composite, the agreement between the two profiles is reasonably good. Comparison between profiles calculated for shorter times, or lower degrees of interaction, showed that there was no significant difference between the profiles. The agreement between 500 hour profiles for the 40 volume percent composite shown in Figure 6 is not as good. In both the 22 and the 40 volume percent composites the superposition profile is higher than the symmetry point profile in the matrix near the filaments. The superposition profile incorrectly shows compositions above the solubility limit of W in Ni. For the symmetry point solution, the interface composition in the matrix is the theoretical solubility limit for the temperature being considered. For the 20 volume percent composite, this error occurs only at or very near the filament/matrix interface, but occurs over nearly half the matrix region for the 40 volume percent composite. The break down of the superposition technique occurs when the tail of the composition profile emanating from a given filament reaches the outer surface of the nearest neighbor filaments. Efforts to employ this method of solution for longer exposure times will result in even larger discrepancies in the matrix region. For a given reaction temperature and time,

the extent of profile overlap will be larger the smaller the filament spacing or the higher the volume fraction filaments. The amount by which the interface composition exceeds the solubility limit of the Ni matrix can be used as an indicator of when solution inaccuracy exceeds acceptable limits.

In comparing the two profiles for the 40 volume percent composite, it will be noted that the filament/matrix interface location predicted by the two different methods of analysis are significantly different. The amount of interface movement calculated by the superposition analysis is erroneously high. The reason for this is that long boundary conditions are used when calculating the single filament profile which is used for superposition. No filament-filament interaction is taken into account. The symmetry point approach does, however, take into account this interaction and correctly slows the rate of interface movement as the composition gradient in the matrix decreases. For this reason the symmetry point analysis should be used for cases where there is a large degree of filament-filament interaction. Superposition can be used for exposure conditions which yield low to moderate degrees of interaction but cannot be accurately used for conditions which yield large degrees of interaction.

Concentration profiles between second nearest neighbor filaments calculated by superposition for a 40 volume percent composite are shown in Figure 7. Curves for exposure times of 10, 100, 200 and 500 hours at 1200^{o}C are presented. There is a progressive filling in of the Ni-matrix and reduction in W-filament diameter with increasing exposure time. The 100 and 200 hour compositional profiles show a small central maxima in the Ni-matrix. Reference to Figure 1 shows that this maxima in the composition profile occurs at point F midway between second nearest neighbor atoms B and D. This maxima is clearly due to

the contributions of filaments A and C which are located adjacent to the central section of the line between second nearest neighbor filaments. For the hexagonal symmetry element being considered, the two filaments located at A and C have a greater contribution to the composition at point F than due the two filaments B and D. The ratio of the distance from C to F to that from D to F is 0.866 which explains the above statement.

It should be noted that the 500 hour composition profile exceeds the solubility limit of W in Ni in the Ni-matrix adjacent to the filaments. This signals break down of the method which means that the 500 hour profile is highly approximate. The extent of interaction is much too large for accurate results to be obtained by superposition.

In order to calculate composition profiles between second nearest neighbors for large degrees of interaction, an alternate method of solution must be employed. Symmetry point analysis can be used to calculate the compositional changes over the end segments of the long body diagonal shown in Figure 1. As discussed in an earlier section, zero flux boundary conditions exist at points E and G. By making this assumption, a direct calculation of the profile from the center of filament D to point E and from the center of filament B to point G is possible. The profiles calculated over these regions for an 0.40 volume fraction W-Ni composite exposed at 1200^{o}C for times of 10, 100, 200 and 500 hours are shown in Figure 8. The central portion, between the minima points in the Ni-matrix, of each profile has been represented by dashed lines to show that they were estimated and not calculated. The symmetry point analysis method does not permit a calculation of the central portion. The composition at the center, point F in Fig. 1 symmetry element, can be determined

because it is just the minimum at the center of the line connecting first nearest neighbor filaments. The central portions of the profiles shown in Figure 8 were obtained by drawing a curve through the calculated central maxima and connecting this curve with the end of the calculated curves at the minima points. Although no mathematical method was used to estimate these curves, a knowledge of what their general shape should be was used in drawing them. The calculated profiles over the end sections, which will generally be the regions of greatest interest, should be reasonably accurate for large degrees of interaction. The same is true for the central maxima point. Thus, although the remainder of the profile had to be estimated, this general approach should give the best profiles possible, particularly for cases of extensive interaction.

A disadvantage of the above approach is the necessity to curve fit the profile over the central region. An attempt was made to calculate the central section by superposition and connect those curves with the end segments calculated by symmetry point analysis. This approach was only moderately successful as exact match-up of the curves was generally not obtained. Typical results for a 40 volume percent composite exposed at 1200^{o}C are plotted in Figure 9. The curves for the central Ni-matrix region were determined by superposition using 174 μm boundary condition finite difference solutions for those plotted in the top graph and 200 μm boundary condition solutions for those plotted in the lower graph. The selection of 174 μm for one boundary condition was due to the fact that 174 μm is one-half the second nearest neighbor distance. The 200 μm boundary condition was selected because it represents a boundary condition long enough that the tail of the 500 hour profile went to zero before reaching that distance from the center of the W-filament.

In general, the central curve segments do not exactly match up with the end segments giving rise to discontinuities in the composite profiles. The magnitude of these discontinuities was small for short times, but became progressively larger with increasing exposure time. Also, the discontinuities are larger for the 200 μm curves (lower plot) than for the 174 μm curves (upper plot).

The center sections shown were calculated by superposition of the contributions from the two closest filaments only (filaments A and C in Figure 1). If the contributions from the four closest filaments (filaments A, B, C and C, Fig. 1) were summed, the curves in the central sections were always higher than the end segments. Also, the curves which resulted by summing the contributions from the four closest filaments were somewhat flatter than those shown in Figure 9. The amount by which they were displaced above the end segments was slightly larger than the negative displacements of the two filament summation profiles. Thus whether the superposition was performed using the contributions from only the two closest or from the four closest filaments match up with the end segments at the minimum points in the matrix was not obtained.

Having considered these approaches to determining profiles between second nearest neighbor filaments let us compare the two most desirable. The 200 hour exposure profiles calculated by superposition and symmetry point analysis shown previously in Figures 7 and 8 are again plotted in Figure 10. Both are plotted on the same graph for ease of comparison. The symmetry point profile is lower than the superposition profile in the nickel matrix regions adjacent to the W-filaments but rises slightly above the superposition profile in the

central region. The superposition profile is clearly too high in the matrix region adjoining the filament as it predicts an interface composition slightly larger than the theoretical solubility limit of tungsten in Ni. Also the superposition technique tends to yield lower values in the center which gives a Ni-matrix profile flatter than would be expected experimentally. The symmetry point analysis is believed to yield the best profiles for the Ni-matrix regions adjoining the filaments. The major disadvantage of this approach, however, is the necessity to estimate the compositions through the central region.

For diffusion times shorter than 200 hours, there was essentially no significant difference between the profiles calculated by the two techniques. However, for diffusion times longer than 200 hours for this particular case, there was a significant difference between the curves calculated by the two methods. This was primarily due to a break down in the superposition technique.

The above discussions have centered on the calculation of compositional changes resulting from interdiffusion in a two phase metal matrix composite system. Besides the variation of composition with distance from the W-filaments, the change in filament volume fraction resulting from interdiffusion can also be obtained. The amount of shift of the filament/matrix interface and corresponding change in filament volume fraction as a function of exposure time at three different temperatures is presented in the two graphs plotted in Figure 11. Corresponding to each temperature, curves for composites containing initial filament volume percents of 6, 22, and 40 are presented. Those curves for which two initial volume fractions are indicated by the numbers at the right signifies that the curves for the two volume fractions shown exactly superimpose. The amount of interface shift reported in the top graph was calculated by symmetry point analysis between first nearest neighbors. The change in

normalized volume fraction with exposure time was calculated for a hexagonal stacking of filaments assuming that there was a uniform reduction in filament diameter corresponding to the amount calculated between nearest neighbor filaments. This is a good assumption for low degrees of filament-filament interaction but is not strictly correct for large degrees of interaction. Examination of the symmetry element shown in Figure 1 in conjunction with the compositional profiles presented in the previous figures will show that the matrix surrounding any filament will not saturate uniformly with time. The region between first nearest neighbor filaments will saturate before the region at the center of the triangle formed by any three filaments. Therefore, for long exposure times, high initial filament volume fraction, and high exposure temperature (1200°C+) where there is extensive interdiffusion, the reported interface shift will be smaller than the average for the filament. Likewise, the reported normalized volume fraction will be higher than the true average. However, for shorter exposure times, lower reaction temperatures, or lower initial filament volume fraction the results presented in Figure 11 are good approximations to the actual values.

The results presented in Figure 11 clearly show the importance of exposure temperature. For the lower temperatures of 1000° and 1100°C, essentially the same interface shift and changes in filament volume fraction was found for composites containing from 0.06 to 0.40 initial volume fraction filaments. This indicates that for these cases the compositional build up in the matrix was not large enough to strongly effect the amount of interface shift. This was not, however, true for the 1200°C exposure condition. For exposure times longer than 200 hours there was a significant difference between the

different volume fraction composites. The higher the filament volume fraction the closer the filaments are spaced which means that compositional build up in the matrix will slow the diffusion process sooner than would be found for lower filament volume fraction composites. The matrix saturates quicker because of the shorter distances through which diffusion takes place and because of the smaller amount of W which can be taken into solution in the Ni matrix.

The above discussions have considered how initial filament volume fraction and exposure temperature affect the change in filament volume fraction with exposure time. The initial filament diameter also has an effect. Curves are presented in Figure 12 which show the change in filament volume fraction with exposure time for composites initially containing 40 and 22 volume percent filaments. Results are presented for initial filament diameters of 20, 40, 60, 100 and 160 μm. The smaller the diameter the larger the number of filaments per unit cross-sectional area and thus the smaller the spacing between filaments. The curves clearly show that the smaller the filament diameter the faster the reduction in filament volume fraction with exposure time. The primary reason for this behavior is the fact that during the early stages of interdiffusion before the matrix begins to saturate, the filament/matrix interface moves approximately the same amount independent of filament diameter. However, a given interface shift produces a much larger percentage drop in filament volume fraction for a small diameter filament composite than in a larger filament composite. The equilibrium filament volume fraction does not depend on filament size but rather depends only on the initial filament volume fraction of the composite. The curves in Figure 12 indicate that this limiting volume fraction will be reached first for a high volume fraction composite containing small

filaments. The apparent lower limits on the filament volume fraction shown in Figure 12 do not correspond to the theoretical limits. The reason for the curves leveling off at a value higher than the theoretical limiting value is related to the scheme used to calculate the reported results. Since the reduction in filament diameter between nearest neighbor filaments was used as the basis for these results, it follows from previous discussions that the limiting volume fraction calculated will be higher than the true value. This method of calculation should, however, give a good approximation of the true filament volume fraction decrease curve up to the point where the curve becomes horizontal. In reality, there would continue to be a slow rate of decrease of the filament volume fraction until the entire Ni matrix was saturated with W. The details of final matrix saturation are not, however, as important from a practical stand point as how fast the initial changes take place. In the early stages of exposure where the most important changes take place, the curves presented in Figure 12 are believed to be reasonably accurate.

To provide an experimental example of the theoretical analysis, a study was undertaken to experimentally measure the compositional and microstructural changes which occur in a W-Ni composite exposed at 1200^{o}C. For this study a composite rod approximately 6 inches long and 3/4 inches in diameter was secured from Battelle Memorial Institute, Columbus, Ohio. This rod was made by vacuum slip casting mickel about a bundle of 5 mil diameter W-filaments. Micrographs of a polishes cross-section of a portion of this rod is shown in Figure 13. The stacking of W-filaments is not regular over the cross-section and there are places where the filaments are touching. There are, however, areas where the local symmetry is similar to that shown in Figure 1 for ideal

hexagonal stacking. The composite consolidation process used to manufacture this sample did result in reaction between the W-filaments and the Ni-matrix. A recrystallization zone in the outer diameter of the W-filaments resulting from diffusion of Ni into the filaments can be seen in the right hand micrograph shown in Figure 13. Because of this interdiffusion, it is necessary to use the electron microprobe to quantitatively measure the extent of interdiffusion. The measured profiles will then be input to the modeling computer program to form the basis for modeling the additional exposure to be given the specimen. The modeling program was written such that the beginning point could be any degree of interdiffusion provided the actual compositional profile existing along the direction of interest is input to the program.

This phase of this program has been held up because the electron microprobe has been broken down. It is anticipated that these studies will be completed in the near future so that the combined results can be submitted for journal publication.

The previous sections clearly demonstrate that the analytical capability to calculate compositional changes in a two-phase metal matrix composite has been developed. Also, an effort is underway to provide an experimental check of these calculations. One major area which has not been considered is concerned with mechanical property changes which occur because of diffusional interaction. Very little work has been reported in the literature on trying to correlate degradation of mechanical properties with compositional and microstructural changes which occur as a result of diffusional processes.

Although this was not originally intended to be done in this study, an initial effort in this direction was started in this investigation. A simplified type of sample consisting of Ni plated on 5 mil diameter wires was selected for the initial study. The objective was to prepare wire specimens

which could be tested in tension as-fabricated and after selected high temperature exposures. This would provide a measure of the amount of degradation in tensile properties resulting from the exposure treatment. The compositional changes in the specimen will be calculated theoretically and experimentally measured. An attempt will then be made to find relationships which correlate the mechanical property changes with the compositional and microstructural changes.

The first stage of this effort requires that the strength properties of the base W-wire be characterized. Also, after electroplating Ni on the W-wire it is again necessary to characterize the resulting strength properties. Several attempts to electroplate the W-wires were required to obtain a deposit with the required properties. Only limited success was achieved in this endeavor and additional work is required to consistantly obtain high quality deposits. The major problem encountered was pitting of the Ni deposit. Several techniques were tried in an attempt to alleviate this problem. The wire was rotated in the solution as well as mechanical agitation of the plating solution. It was not determined whether the pitting was due entirely to gas evolution on the plating surface or to lack of complete activation of the original W surface. Additional work is required to overcome this and other plating difficulties encountered in the production of samples of high quality.

Fractographs of a W-wire and a Ni-plated W-wire loaded uniaxially to failure are shown in Figure 14. The general appearance of the W-wire fracture surface suggests a ductile mode of fracture. Cracking of the W-wire can be noted in the fractographs. The appearance of the Ni-plating fracture surface suggest a much more brittle type of fracture. It is well known that Ni electrodeposits may show a low amount of ductility depending on the plating bath and operating conditions used. The ductility of this particular deposit

was low because of less than optimum plating conditions. As noted above, these results are only preliminary and more work is required before meaningful trends and strength properties of as-plated wires can be determined.

A limited number of exposure tests were conducted at 1200°C even though the sample preparation problems had not been completely solved. Fractographs of two Ni-plated W-wires loaded uniaxially to failure after exposure at 1200°C for 2 hours and 5 hours in dry nitrogen are shown in Figure 15. Examination of these fractographs reveals that diffusional interaction has caused complete recrystallization of the W-wire after 5 hours and partial recrystallization after the 2 hour exposure. Recrystallization of the W occurs first in the outer part of the wire adjacent to the Ni plating and is caused by diffusion of Ni into the W-wire. The exact mechanism by which Ni diffusion into the W causes recrystallization is not known. The presence of the recrystallized layer greatly lowers the strength of the W-wire and results in a brittle type of failure. It is also known that there is a ductile to brittle transition in this system and these tests conducted at room temperature were below the transition temperature. Additional tests above the transition temperature are planned once good quality specimens are available.

Considerable additional work is required to understand all of the changes which occur as a result of diffusional interactions. The effect of structural and compositional changes on the mechanical properties will require a systematic study of composition, microstructure, and properties. The knowledge to be gained from such a study would be of importance in understanding how well a given hardware component made of composite material would perform in service.

SUMMARY AND CONCLUSIONS

This study has shown that interdiffusion between filaments and matrix in a two phase metal matrix composite system can be analytically treated. Compositional changes were calculated for an example two-phase composite system, W-filaments/Ni-matrix, over the 1000° to 1200°C temperature range. Two different methods for calculating compositional changes between first and second nearest neighbor filaments have been considered. Symmetry point analysis was used to calculate composition profiles along lines of "high" symmetry where zero flux boundary conditions could be defined. This technique can be used to treat low or high degrees of interaction provided appropriate boundary conditions can be defined. Superposition was also used to calculate compositional changes. This approach has the advantage of being generally applicable along any line through the composite. It gives good results for low to moderate degrees of interaction but can not be used for cases where there is extensive interdiffusion. For short exposure time, or low degrees of interaction, there was essentially no significant difference between the first nearest neighbor profiles calculated by superposition or symmetry point analysis.

The calculation of compositional changes in the composite also yielded information on the change in filament volume fraction with exposure time. The effect of initial filament diameter and initial filament volume fraction on the rate of decrease in filament volume fraction for given exposure conditions was also determined. Results are presented for three different temperatures to illustrate the importance of temperature on the diffusion processes.

The general success of the finite-difference model as a predicative tool for two-phase binary composite systems suggest that the development of such models for treating more complex composite systems may also prove useful.

LIST OF FIGURE CAPTIONS

Figure 1. Idealized arrangement of filaments in a metal matrix composite.

Figure 2. Schematic cross-section of diffused two-phase composite showing filament/matrix interface and definition of parameters used in finite difference analysis.

Figure 3. Concentration profiles for a single W-filament embedded in a Ni-matrix and exposed at 1200°C.

Figure 4. Concentration profiles between nearest neighbor filaments in a (a) 22 and (b) 40 volume percent W-filament composite exposed at 1200°C.

Figure 5. Comparison of concentration profiles calculated between nearest neighbor filaments for exposure at 1200°C and 1100°C for 200 hrs.

Figure 6. Comparison of nearest neighbor profiles calculated by superposition and symmetry point analyses.

Figure 7. Concentration profiles between second nearest neighbor filaments calculated by employing superposition.

Figure 8. Concentration profiles between second nearest neighbor filaments calculated by the symmetry point analysis.

Figure 9. Second nearest neighbor profiles determined by employing superposition with a (a) 174 μm b. C. Sol. and (b) 200 μm b. C. Sol. for the center section and symmetry point analysis for the end sections.

Figure 10. Comparison of second nearest neighbor profiles calculated by employing superposition and symmetry point analyses.

Figure 11. Shift of W/Ni interface and change in filament volume fraction as a function of exposure time at three different temperatures.

Figure 12. Change in filament volume fraction with exposure time at 1200°C for composites containing different size filaments.

Figure 13. Scanning electron micrographs of a polished cross-section of an as-received W/Ni composite specimen.

Figure 14. Cross-section of a (a) W-wire and a (b) Ni-plated W-wire loaded uniaxially to failure.

Figure 15. Cross-sections of Ni-plated W-wires loaded uniaxially to failure after exposure to 1200°C for 2 hours (a), (b) and 5 hours (c), (d).

REFERENCES

1. A. Metcalfe: Interfaces in Metal Matrix Composites, Vol. 1, p. 5, Academic Press, New York, 1974.

2. H. W. Herring and D. R. Tenney: Met. Trans., 1973, Vol. 4, pp. 437-41.

3. D. Murray and F. Landis: Trans. AIME, Ser. D, 1959, Vol. 81, pp. 106-12.

4. R. A. Tranzilli and R. W. Heckel: Trans. TMS-AIME, 1968, Vol. 242, pp. 2313-21.

5. R. A. Tranzilli and R. W. Heckel: Trans. TMS-AIME, 1969, Vol. 245, pp. 1363-66.

6. R. A. Tranzilli and R. W. Heckel: Met. Trans. 1971, Vol. 2, pp. 1779-84.

7. A. G. Guy, R. T. DeHoff, and C. B. Smith: Trans. ASM, 1968, Vol. 61, p. 314.

8. J. W. Colby: Advances in X-Ray Analysis, Vol. 11, p. 287, Plenum Press, 1968.

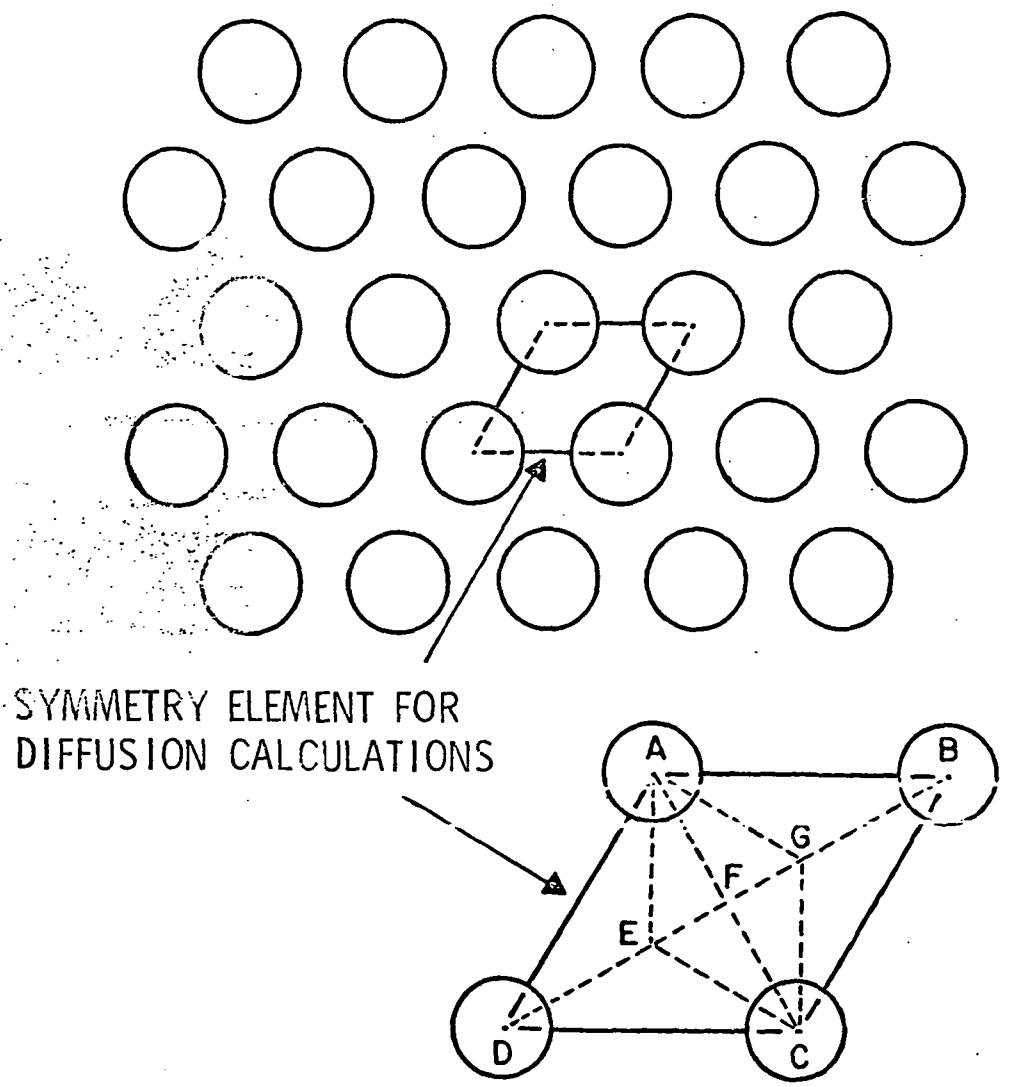

Figure 1. - Idealized arrangement of filaments in a metal matrix composite.

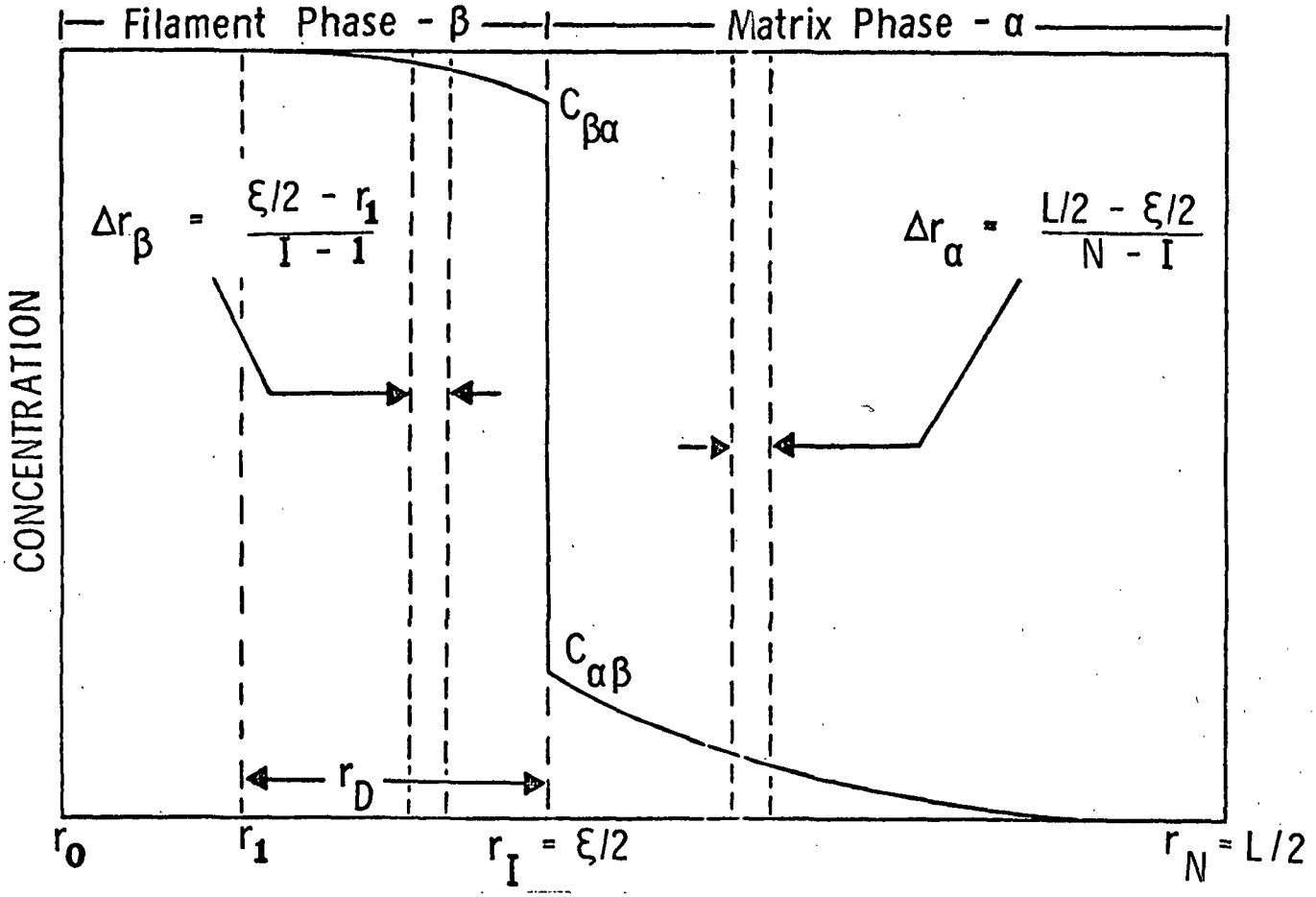

Figure 2. - Schematic cross-section of diffused two-phase composite showing filament/matrix interface and definition of parameters used in finite defference analysis.

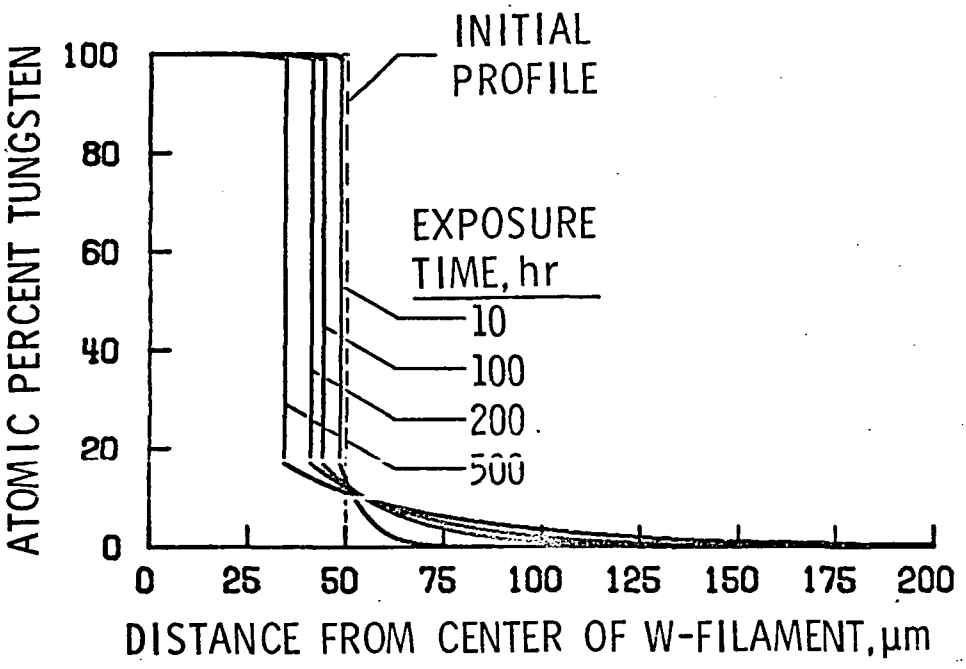

Figure 3. - Concentration profiles for a single W-filament embedded in a Ni-matrix and exposed at 1200C.

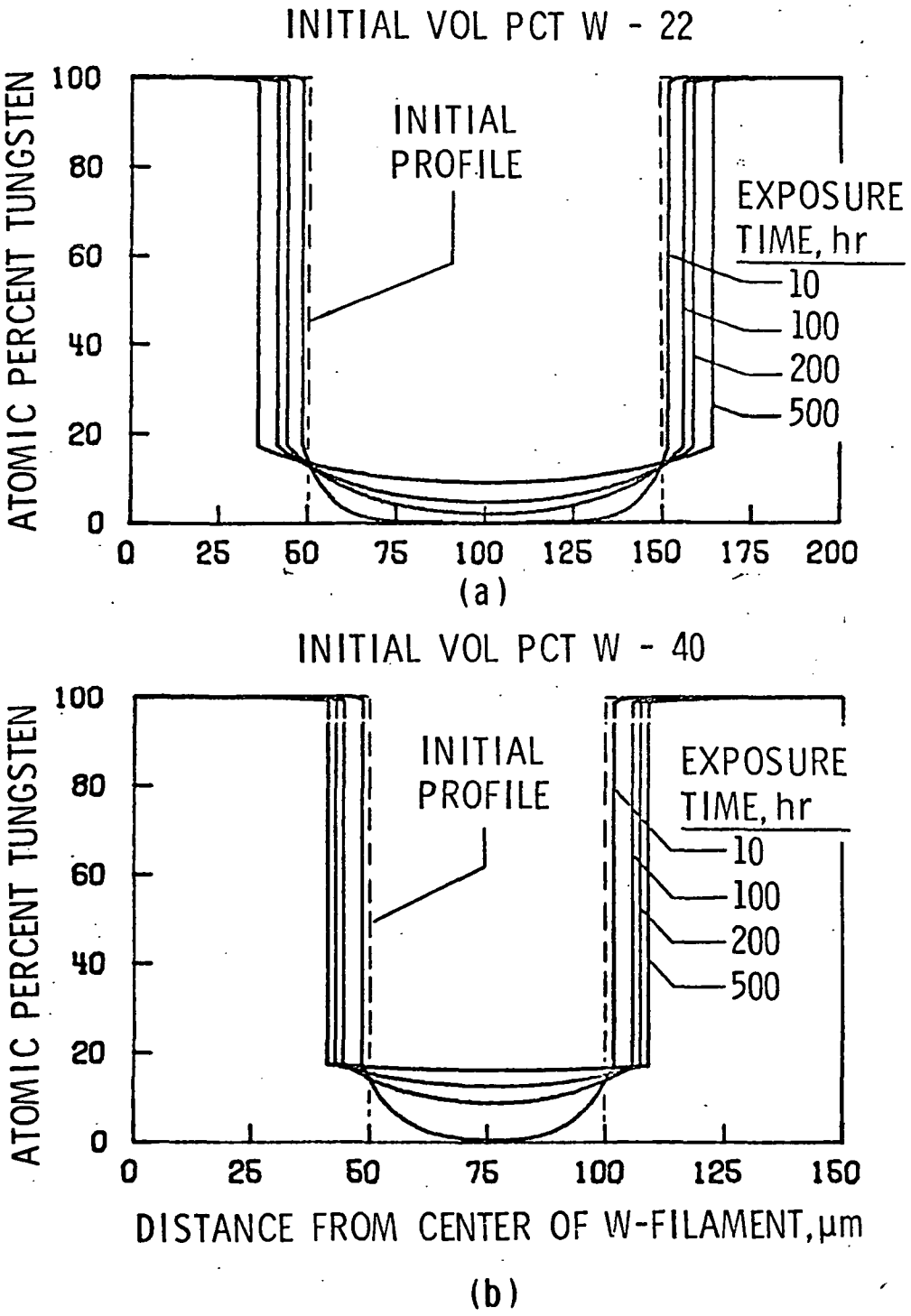

Figure 4. - Concentration profiles between nearest neighbor filaments in a (a) 22 and (b) 40 volume percent W-filament composite exposed at 1200C.

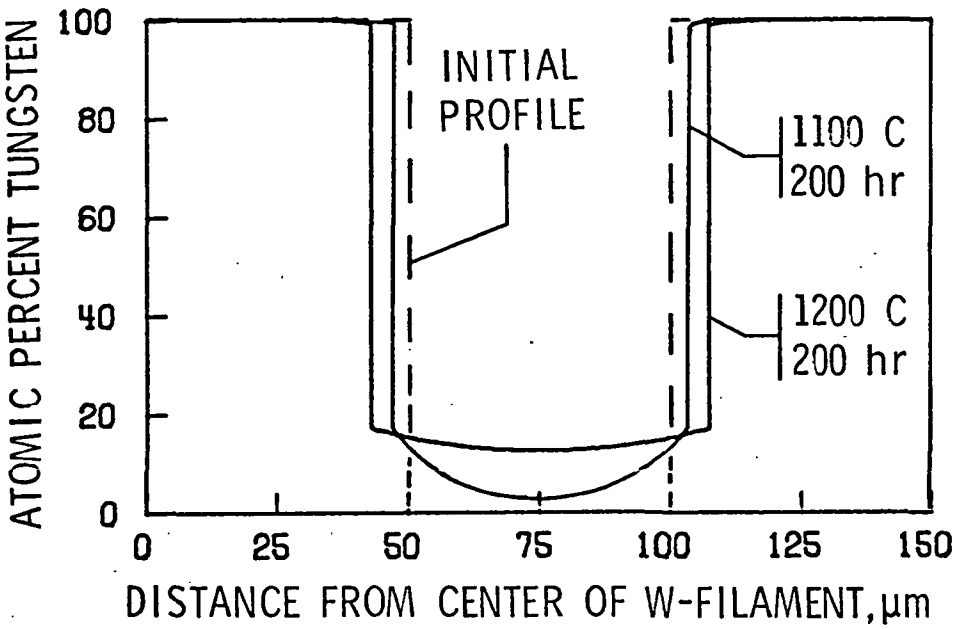

Figure 5. - Comparison of concentration profiles calculated between nearest neighbor filaments for exposure at 1200C and 1100C for 200 hrs.

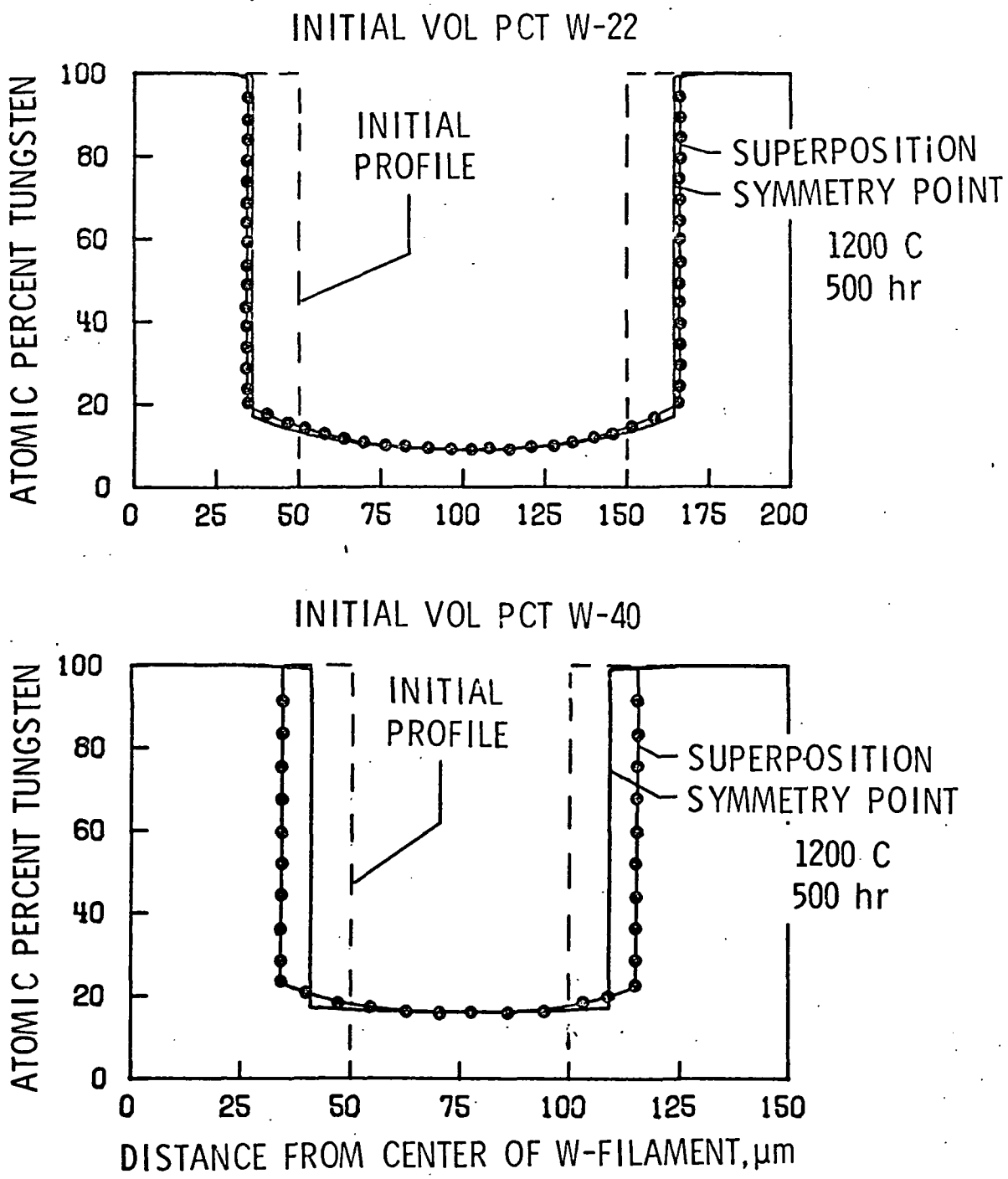

Figure 6. - Comparison of nearest neighbor profiles calculated by superposition and symmetry point analyses.

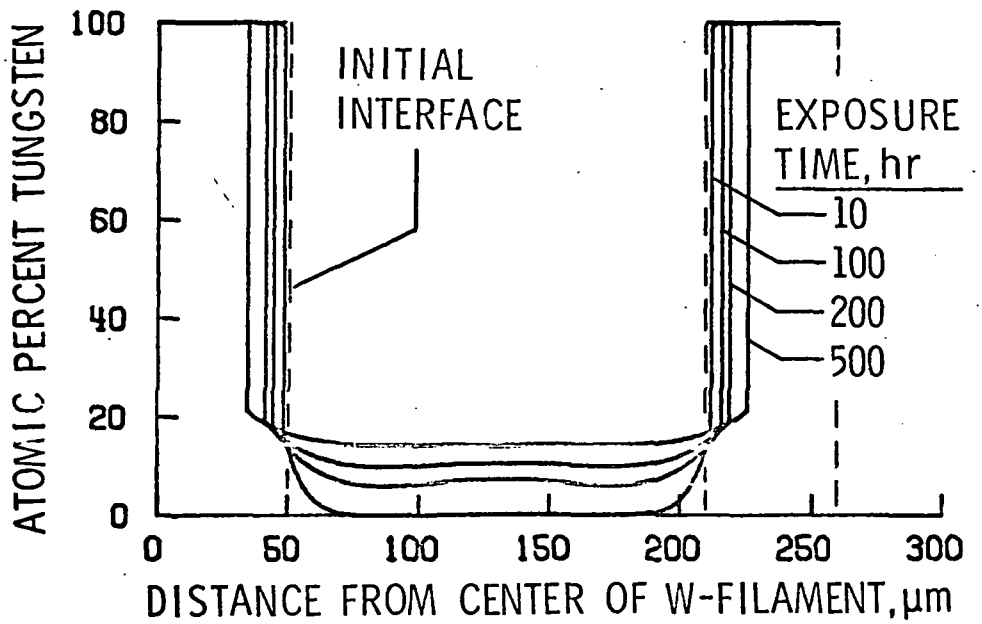

Figure 7. - Concentration profiles between second nearest neighbor filaments calculated by employing superposition.

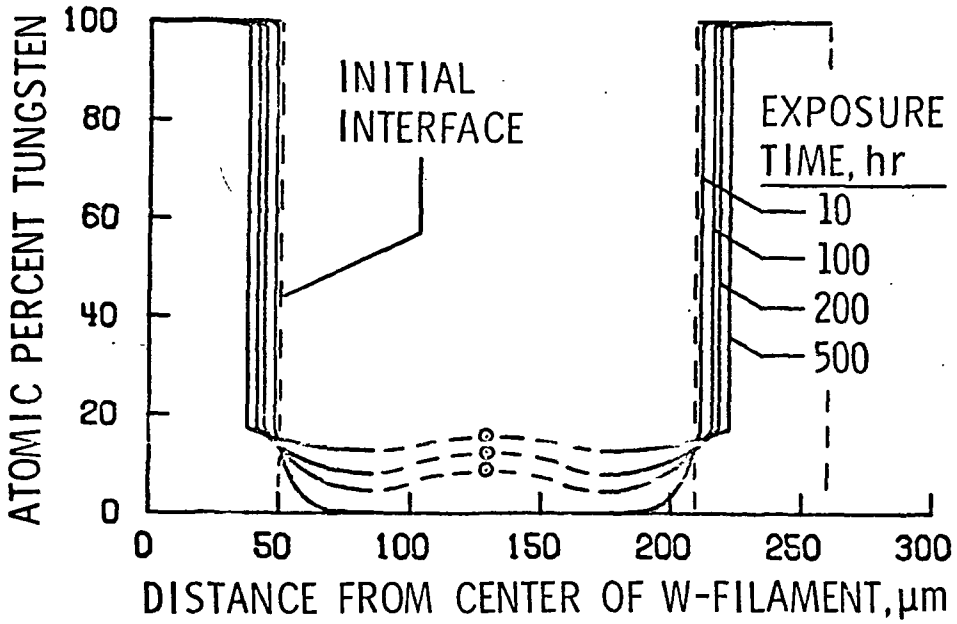

Figure 8. - Concentration profiles between second nearest neighbor filaments calculated by the symmetry point analysis.

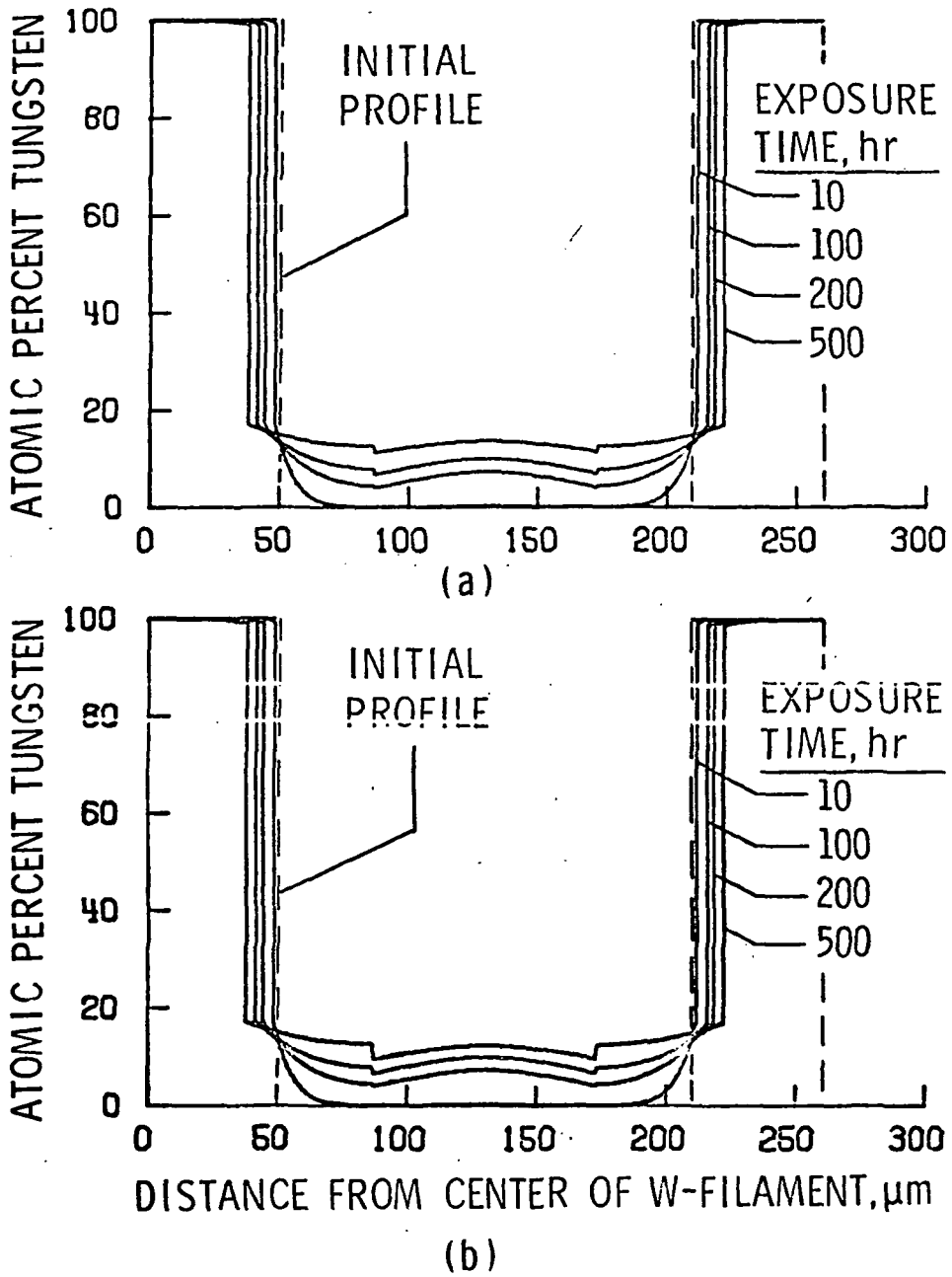

Figure 9. - Second nearest neighbor profiles determined by employing superposition with a (a) 174μm b.c. sol. and (b) 200μm b.c. sol. for the center section and symmetry point analysis for the end sections.

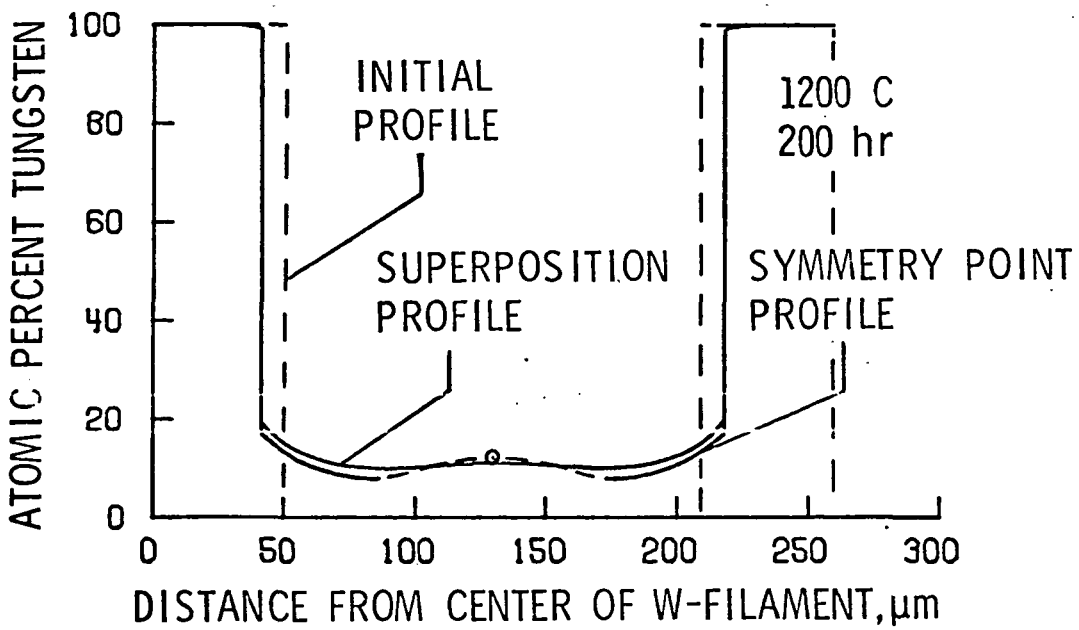

Figure 10. - Comparison of second nearest neighbor profiles calculated by employing superposition and symmetry point analyses.

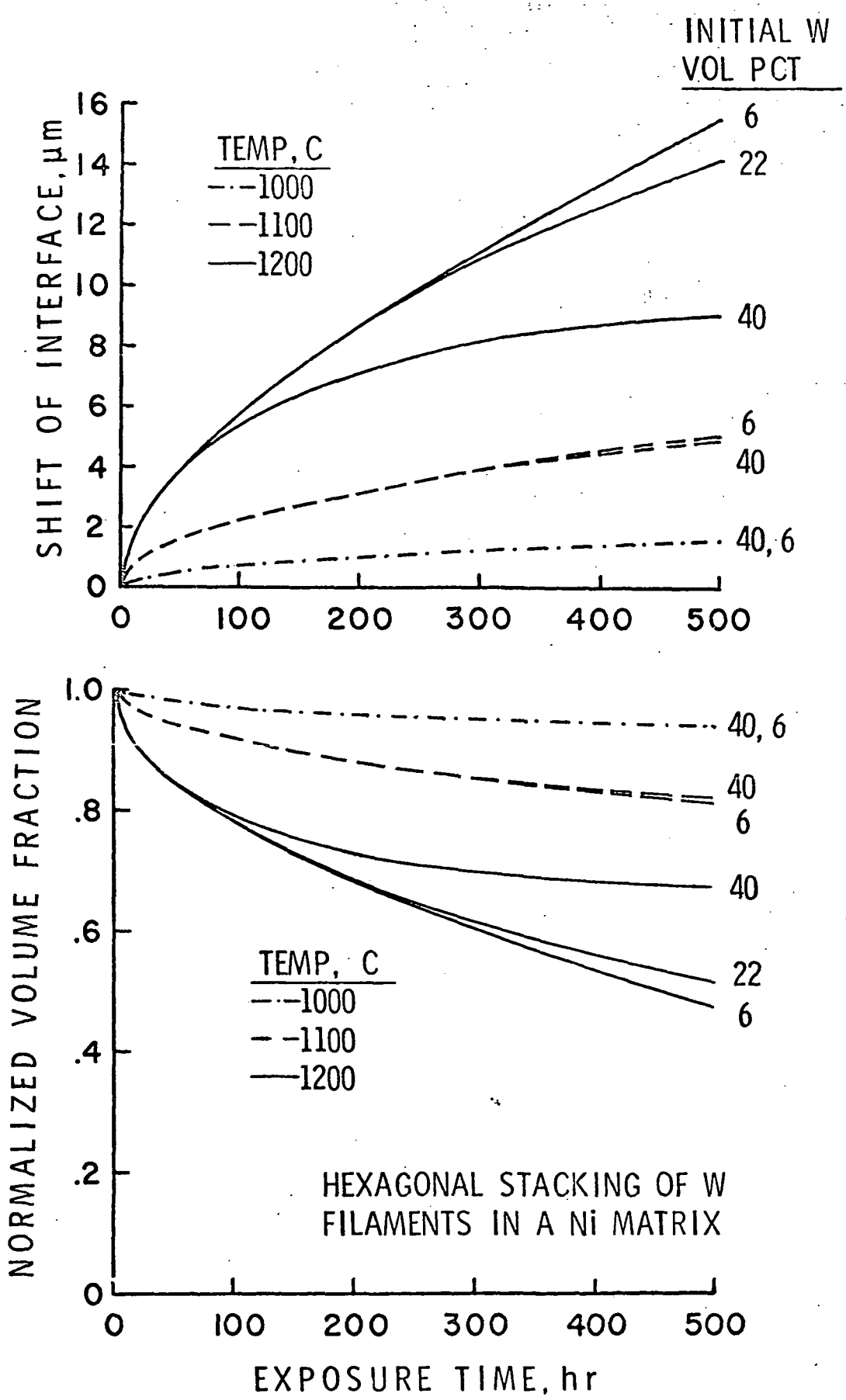

Figure 11. - Shift of W/Ni interface and change in filament volume fraction as a function of exposure time at three different temperatures.

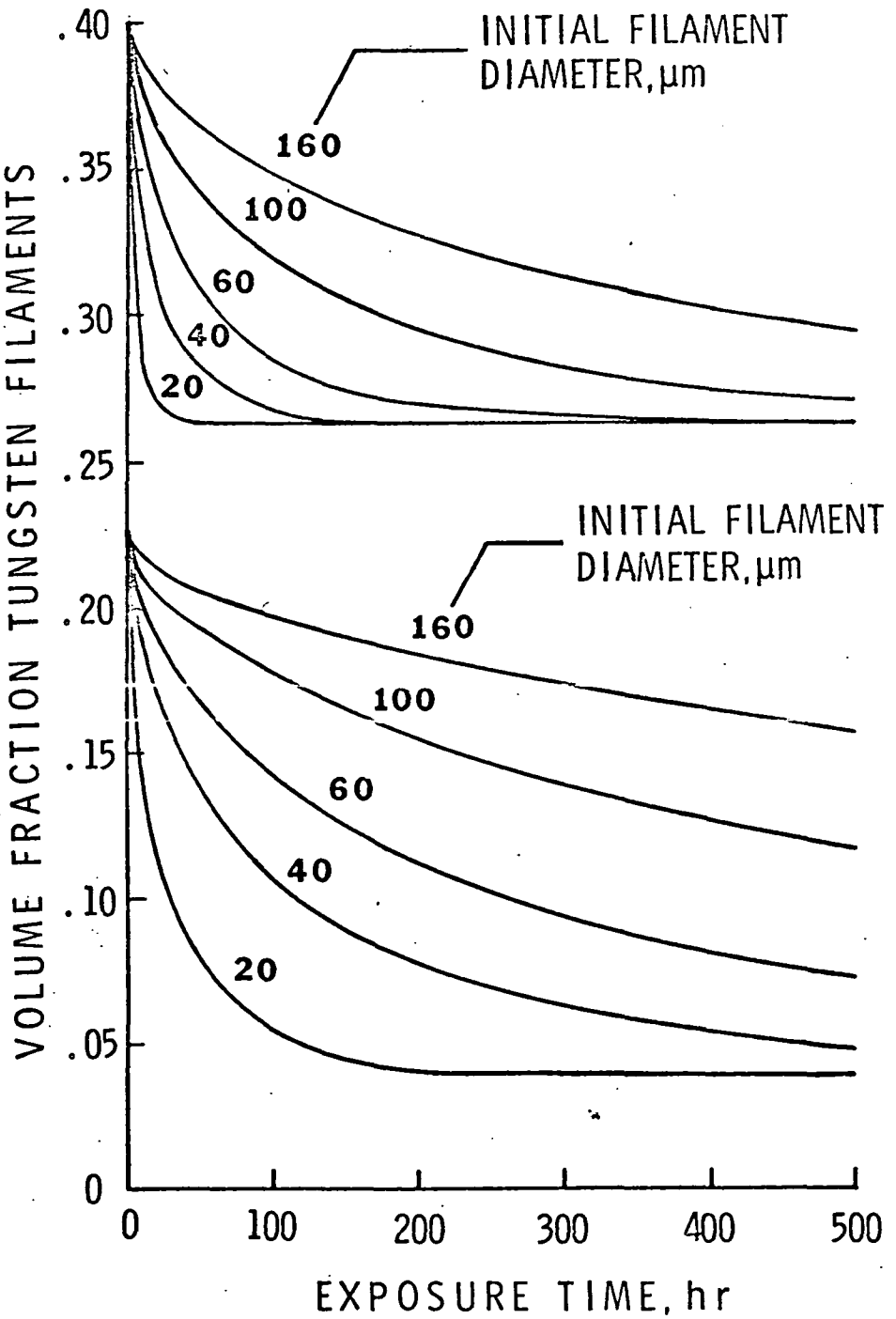

Figure 12. - Change in filament volume fraction with exposure time at 1200 C for composites containing different size filaments.

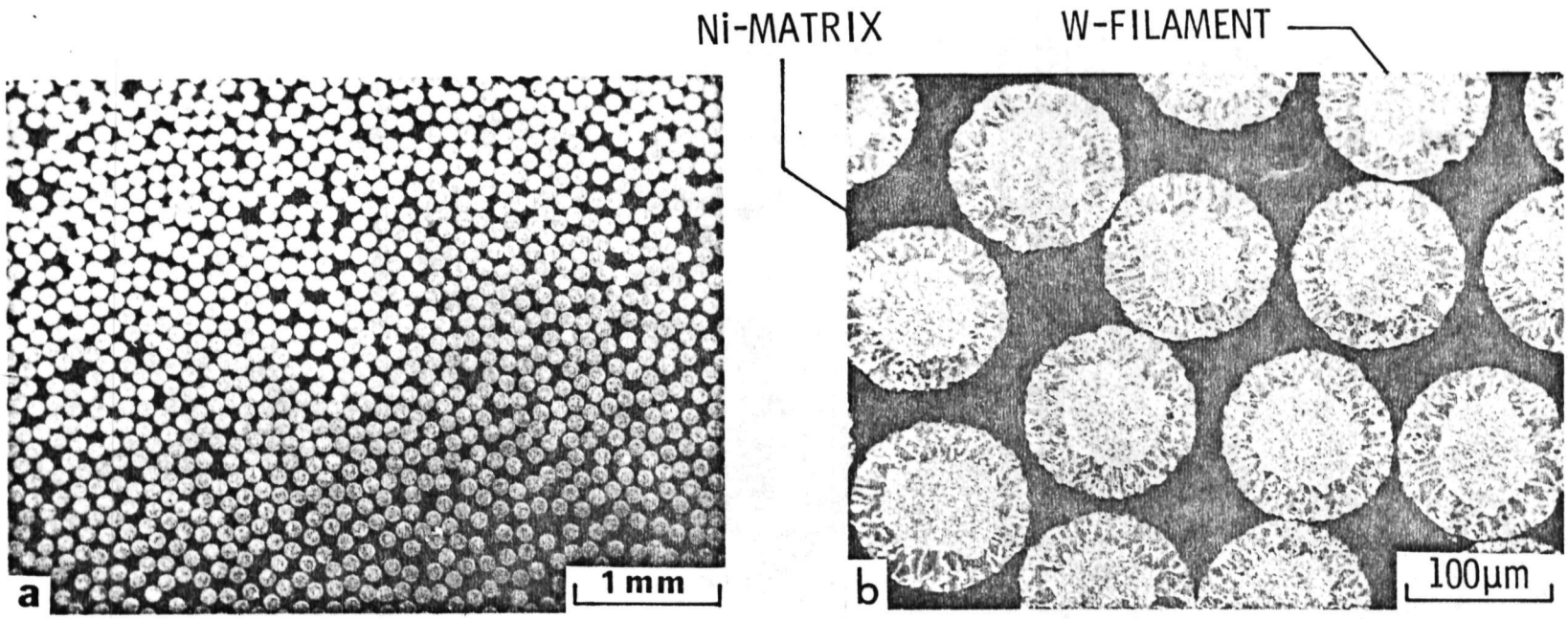

Figure 13. - Scanning electron micrographs of a polished cross-section of an as-received W/Ni composite specimen.

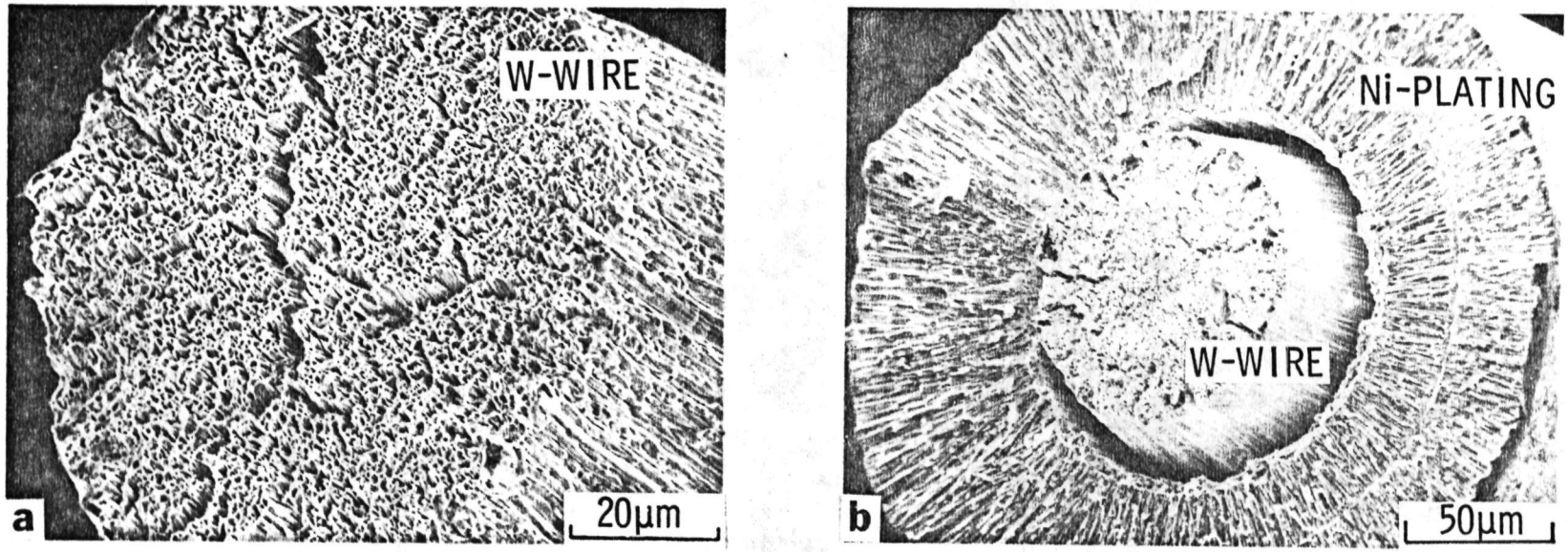

Figure 14. - Fractographs of a (a) W-wire and (b) Ni-plated W-wire loaded uniaxially to failure.

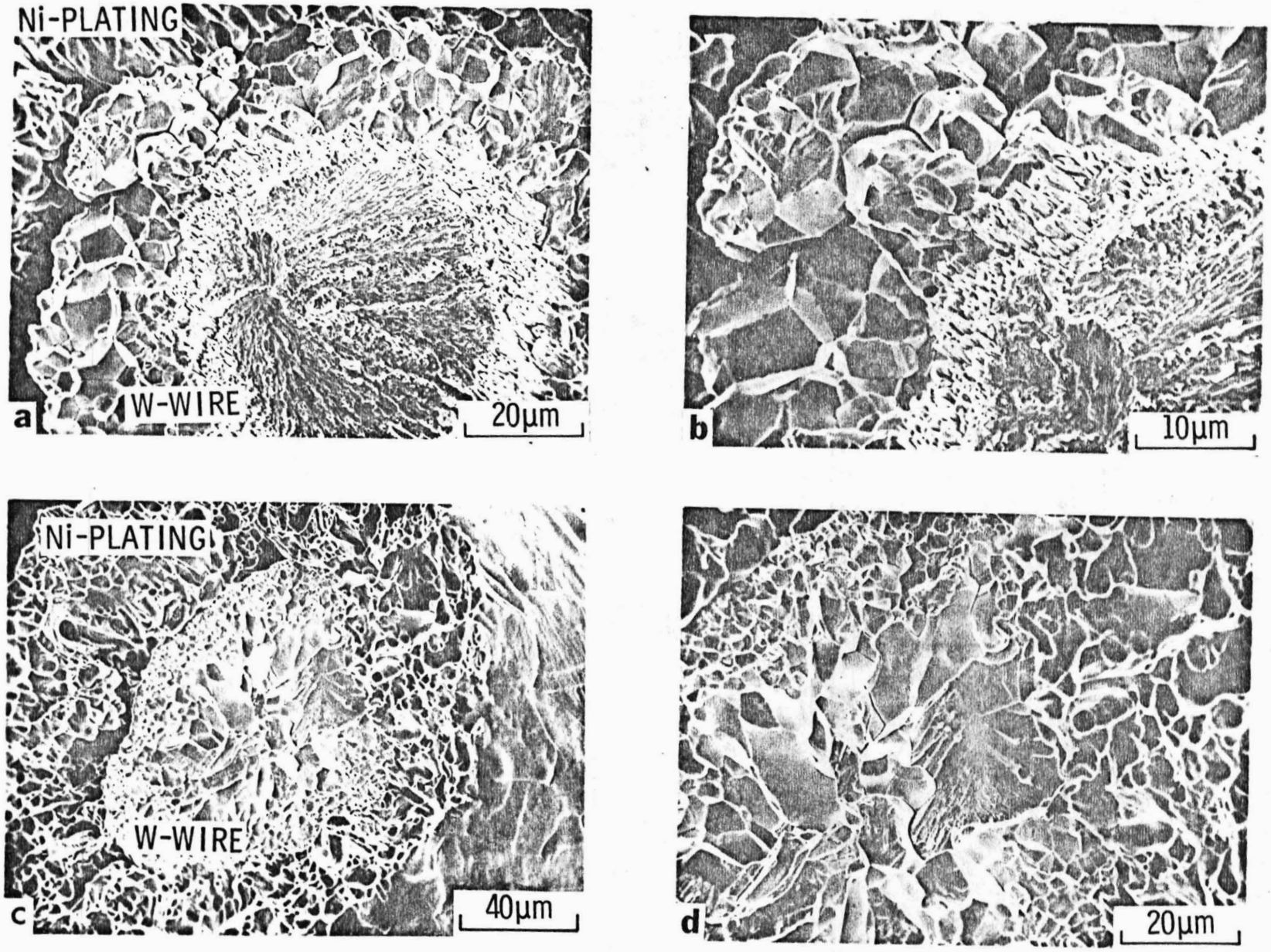

Figure 15. - Fractographs of Ni-plated W-wires loaded uniaxially to failure after exposure to 1200 C for 2 hrs. (a), (b), and 5 hrs. (c), (d).